The Canadian Mineralogist
Vol. 42, pp. 155-168 (2004)

THE PARAGENESIS OF PYROPHANITE FROM SIERRA DE COMECHINGONES, CÓRDOBA, ARGENTINA

FEDERICA ZACCARINI [§] AND GIORGIO GARUTI

Dipartimento di Scienze della Terra, Università di Modena e Reggio Emilia, Via S.Eufemia, 19, I-41100 Modena, Italy

ARIEL ORTIZ-SUAREZ AND ANDRES CARUGNO-DURAN

Departamento de Geología, Universidad Nacional de San Luis, Chacacabuco, 5700 San Luis, Argentina

ABSTRACT

Pyrophanite ($MnTiO_3$) has been discovered for the first time in Argentina, associated with metamorphosed Fe ore in the Sierra de Comechingones, Province of Córdoba. The Fe ore mainly consists of magnetite, and contains large grains of Ti-rich magnetite, showing a complex unmixing assemblage composed of pyrophanite, manganoan ilmenite, an aluminous spinel, and hematite. The gangue minerals associated with the oxides are, in order of decreasing abundance, clinopyroxene, garnet, titanite, amphibole, clintonite, calcite, chlorite, quartz and rare epidote. Electron-microprobe analyses show extensive solid-solution among the end-members pyrophanite, ilmenite, and geikielite ($MgTiO_3$). The unmixed assemblage may have been derived from oxidation of a former Mn–Mg-rich magnetite–ulvöspinel solid solution, under metamorphic conditions. The lack of Mn in the silicate gangue associated with the Fe ore excludes the possible influence of Mn-rich fluids during metamorphism, and suggests that Mn was an important constituent of the original oxide protolith. Geothermometry applied to the chlorite associated with the oxides yielded temperatures as low as 300–350°C, possibly consistent with the closure of the metamorphic system. However, textural and mineralogical evidence suggest that the temperature of metamorphism was much higher, and possibly reached a stage of partial melting.

Keywords: pyrophanite, magnetite, ilmenite, clintonite, chlorite, Sierra de Comechingones, Argentina.

SOMMAIRE

Nous avons trouvé la pyrophanite ($MnTiO_3$) en association avec un minerai de fer métamorphisé à Sierra de Comechingones, province de Córdoba; c'est la première fois que ce minéral est signalé en Argentine. Le minerai, à prédominance de magnétite, contient aussi des grains grossiers de magnétite titanifère qui fait preuve d'une démixion complexe, menant à un assemblage de pyrophanite, ilménite manganifère, un spinelle alumineux, et hématite. Les minéraux de la gangue associés aux oxydes sont, classés selon leur abondance, clinopyroxène, grenat, titanite, amphibole, clintonite, calcite, chlorite, quartz et, plus rarement, épidote. Les analyses à la microsonde électronique révèlent une étendue marquée de solution solide impliquant les pôles pyrophanite, ilménite, et geikielite ($MgTiO_3$). Cet assemblage de démixion pourrait avoir été dérivé d'une oxydation d'un précurseur comme une solution solide magnétite–ulvöspinelle riche en Mn et Mg, sujet à des conditions métamorphiques. L'absence de Mn dans la gangue silicatée associée au minerai de fer semble exclure l'influence d'une phase fluide riche en Mn au cours du métamorphisme, et semble plutôt indiquer que le manganèse était important dans l'oxyde précurseur. La géothermométrie fondée sur la chlorite indique des températures de l'ordre de 300–350°C, peut-être réalistes pour le stade ultime du métamorphisme. Toutefois, d'après les critères texturaux et minéralogiques, la température de métamorphisme était considérablement supérieure, et aurait peut-être même atteint un stade de fusion partielle.

(Traduit par la Rédaction)

Mots-clés: pyrophanite, magnétite, ilménite, clintonite, chlorite, Sierra de Comechingones, Argentine.

[§] *Present address*: Institute of Geological Sciences, University of Leoben, Peter Tunner Straße 5, A-8700 Leoben, Austria. *E-mail address:* fedezac@tsc4.com

Introduction

Pyrophanite, $MnTiO_3$, is a rarely encountered member of the ilmenite group. It was discovered in the manganese ore of the Harstig mine, Pajsberg, Sweden (Hamberg 1890). By the end of the forties, only two other localities were found, in Brazil (Derby 1901, 1908) and in Wales (Smith & Claringbull 1947). At present, more than thirty occurrences are known world-wide, and in most of them, pyrophanite is associated with sedimentary or metamorphosed manganese deposits. Pyrophanite has also been discovered in epithermal and hydrothermal manganese deposits. Furthermore, pyrophanite was found associated with metamorphosed zinc- and manganese-rich deposits. Occasionally it has been encountered in banded iron formation. Pyrophanite may also occur associated with gneisses, granitic rocks, alkaline complexes and carbonatites. It has also been reported to occur in serpentinites and even in meteorites (Petaev *et al.* 1992, Krot *et al.* 1993).

In spite of the impressive number of new reports of pyrophanite, only a few of them give a detailed description of its composition and the phase relations of the mineral. To the best of our knowledge, pyrophanite has never been found in Argentina. In this paper, we report the first information about pyrophanite from Sierra de Comechingones, Province of Córdoba, and provide an extended set of electron-microprobe data on pyrophanite and the associated oxides and silicates, along with observations on paragenesis and phase relations. The composition of pyrophanite from Sierra de Comechingones is compared with chemical data from other occurrences worldwide reported in the literature. The data obtained are used to better define the chemical–physical conditions in the metamorphic rocks of Sierra de Comechingones that led to the formation of pyrophanite and its associated minerals.

Geological Background and Information About the Samples

The Sierras de Córdoba (Fig. 1) is located in central Argentina between latitude 30° and 33° South. Its general geological setting corresponds to a low-angle subduction zone in which a series of basement blocks up-welled during the Andean orogenesis (Isacks 1988, Jordan & Allmendinger 1986). The crystalline basement is mainly composed of different metamorphic rocks, such as migmatites, gneisses, minor marble and amphibolites, intruded by Paleozoic granites with small amounts of mafic–ultramafic rocks units (Gordillo & Lencinas 1979). The metamorphic rocks are related to various events that took place between the Precambrian and the lower Paleozoic (Kraemer *et al.* 1995) or between the Cambrian and the Ordovician (Rapela *et al.* 1998, Sims *et al*. 1998). Occasionally, the basement rocks are covered by Upper Paleozoic to Cenozoic sedimentary units and Cretaceous to Tertiary volcanic units (Gordillo & Lencinas 1979).

Pyrophanite was discovered in mafic–ultramafic rocks of Sierra de Comechingones (southern Sierras de Córdoba) at latitude 32°26' South and longitude 64°34' West (Fig. 2). The mineral is part of an oxide assemblage constituting lenses of Fe ore associated with a polymetamorphic sequence of serpentinite, amphibolite, gneisses, minor marble and pegmatite dykes (Guereschi & Baldo 1993, Guereschi & Martino 2002, 2003). Gabbros and granites are the only intrusive igneous rocks in the area. The pyrophanite-bearing samples were collected in one small pit (5 × 2 m) dug for exploration. Unfortunately, field relationships of the orebodies with their host rocks are not exposed in the pit and could not be unequivocally established by surface exploration of the surrounding area because of the strong metamorphic overprint and intense deformation.

Analytical Methods

Eleven polished sections and five thin sections were obtained from eight samples of the Fe ore, and were studied by both reflected and transmitted light microscopy. Pyrophanite and the associated minerals were analyzed with an electron microprobe at the University of Modena and Reggio Emilia, using an ARL–SEMQ instrument, operated at an excitation voltage of 15 kV and a beam current of 15 nA. The detection limits for each element sought, as well as corrections for the interferences, were automatically established with the updated version 3.63, January 1996, of the PROBE software (Donovan & Rivers 1990). Natural albite, microcline, clinopyroxene, olivine, chromite, ilmenite and spessartine were used as standards. The *K*α X-ray lines were used for all the elements of interest. The ferric iron content of oxide minerals was calculated from ideal stoichiometry.

Petrography of the Fe Ore

On the scale of the hand sample, the Fe ore consists of oxides arranged in millimetric bands alternating with the gangue minerals in a proportion of about 50% by volume. Results of the microscope study show that the ore-mineral assemblage is dominated by magnetite, accompanied by ilmenite, pyrophanite, green spinel and rare hematite, whereas sulfides are absent. The gangue minerals associated with the oxides are, in order of decreasing abundance, clinopyroxene, garnet, titanite, amphibole, clintonite, calcite, chlorite, quartz and rare epidote. The oxide–gangue relationships indicate equilibrium recrystallization of the mineral assemblage under metamorphic conditions, with formation of mosaic textures, development of near-120° triple junctions (Fig. 3A). The texture also displays reciprocal inclusions of oxides and silicates and an atoll-shape intergrowth of

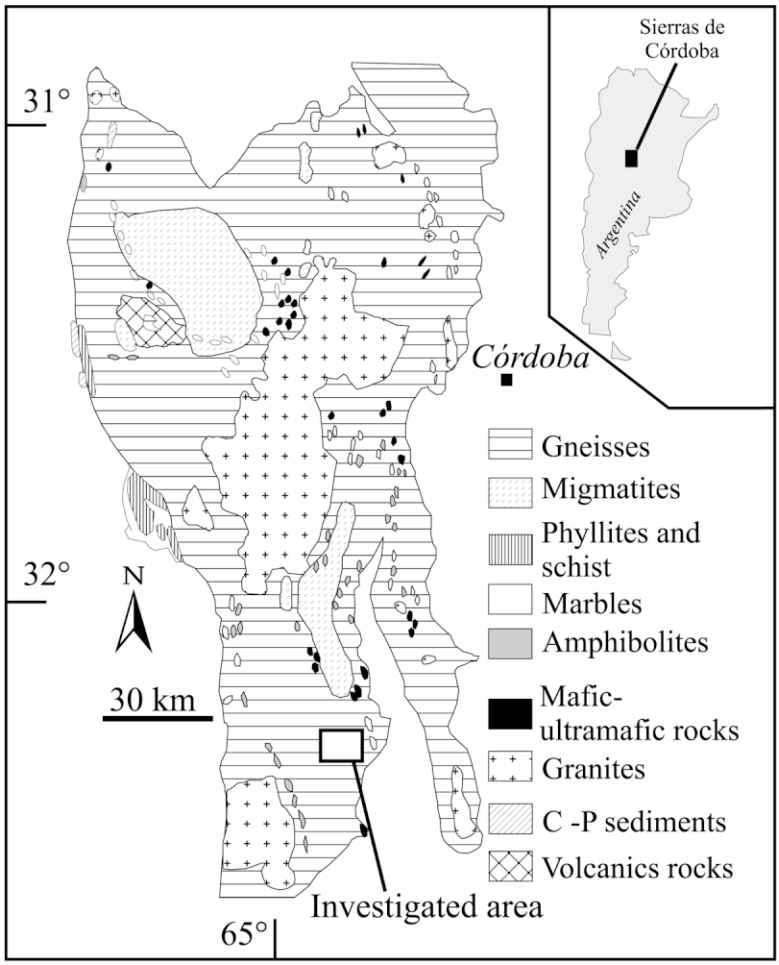

FIG. 1. Simplified geological sketch-map of a portion of the Sierras de Córdoba showing the location of the investigated area (based on Kraemer *et al.* 1995).

the oxide minerals with lobate boundaries, as a result of metamorphic cocrystallization (Fig. 3B).

Magnetite is the most common oxide, followed in order of abundance by Ti-rich magnetite. The latter is clearly distinguished from normal magnetite because of its lower reflectance and because of the ubiquitous presence of exsolution lamellae of ilmenite-series minerals and aluminous spinel. Pyrophanite and ilmenite occur exclusively associated with Ti-rich magnetite in the form of lamellae and as a partial corona at the rim of grains of Ti-rich magnetite (Fig. 4). The aluminous spinel systematically occurs in the coronas, the texture indicating that the mineral is part of the exsolution assemblage, although it has been observed also as free grains in the gangue matrix of the Fe ore. Hematite forms lamellae in normal magnetite, arranged in a geometric pattern reflecting (111) crystallographic planes of the mineral host, as typical in "martite" replacement textures (Fig. 3B). Clinopyroxene, typically with a mosaic texture, is the major constituent of the gangue (Fig. 3A). Garnet appears either as idiomorphic crystals (Fig. 4B) or large poikilitic plates including clinopyroxene and oxides (Figs. 4C, D). Garnet also occur included in the oxides (Figs. 4A, B, D, E). Titanite usually occurs as large lobate grains associated with the oxide minerals (Fig. 3B). Calcite, quartz, chlorite and clintonite are encountered as minor or accessory minerals randomly distributed in the gangue matrix.

THE COMPOSITION OF PYROPHANITE AND ASSOCIATED MINERALS

The pyrophanite has reflected-light properties very similar to those of ilmenite. It shows a distinct

bireflectance from bluish grey to grey and strong anisotropy varying from grey to brownish grey. Internal reflections were not observed. One can distinguish the two phases only on the basis of chemical data. Representative results of electron-microprobe analyses of pyrophanite, ilmenite and the other associated oxides are presented in Table 1. Reciprocal variations of the major oxides MnO, FeO and MgO are shown in Figure 5. The oxides MnO and FeO show clear negative correlation as a result of a complete range of solid solution from ilmenite $(Fe_{0.9}Mn_{0.1})TiO_3$ to pyrophanite $(Fe_{0.2}Mn_{0.8})TiO_3$, the compositional variation being independent of their location, be it in lamellae or coronas. Their Mg content is invariably lower than 6 wt% MgO, and none of the compositions enters the field of geikielite ($MgTiO_3$). The highest Mg contents (> 4 wt% MgO) are found in one group of intermediate compositions between manganoan ilmenite, $(Fe_{0.7}Mn_{0.2}Mg_{0.1})TiO_3$, and ferroan pyrophanite, $(Fe_{0.3}Mn_{0.4}Mg_{0.3})TiO_3$. The reason for the behavior of Mg is not understood, although it would appear to be independent of textural development.

Magnetite is pure Fe_3O_4 with trace amounts of Ti (<0.2 wt% TiO_2), Mn, Mg, and Al. The titaniferous

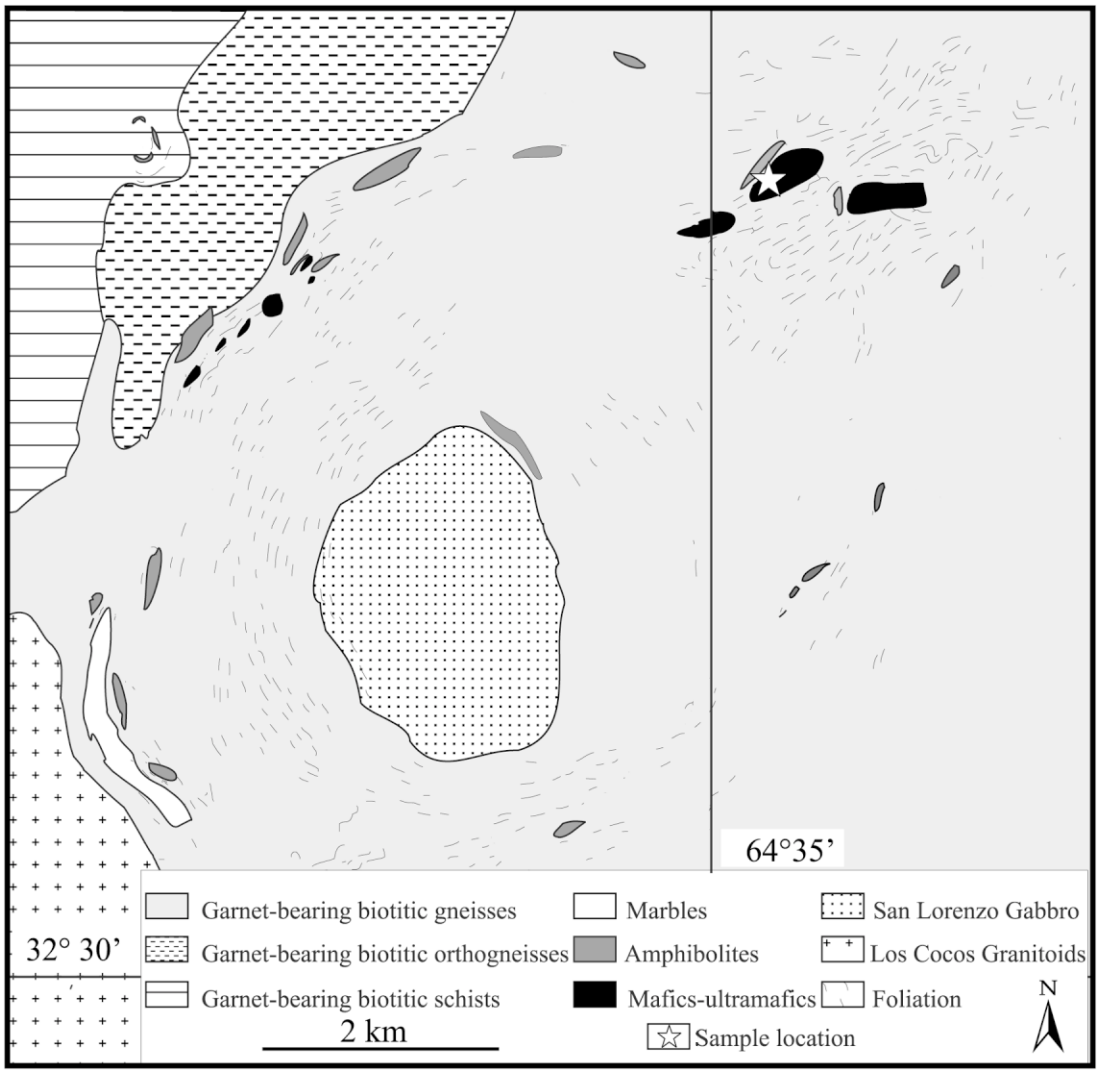

FIG. 2. Geological sketch-map of the Sierra de Comechingones (modified after Guereschi 2000) and sample location.

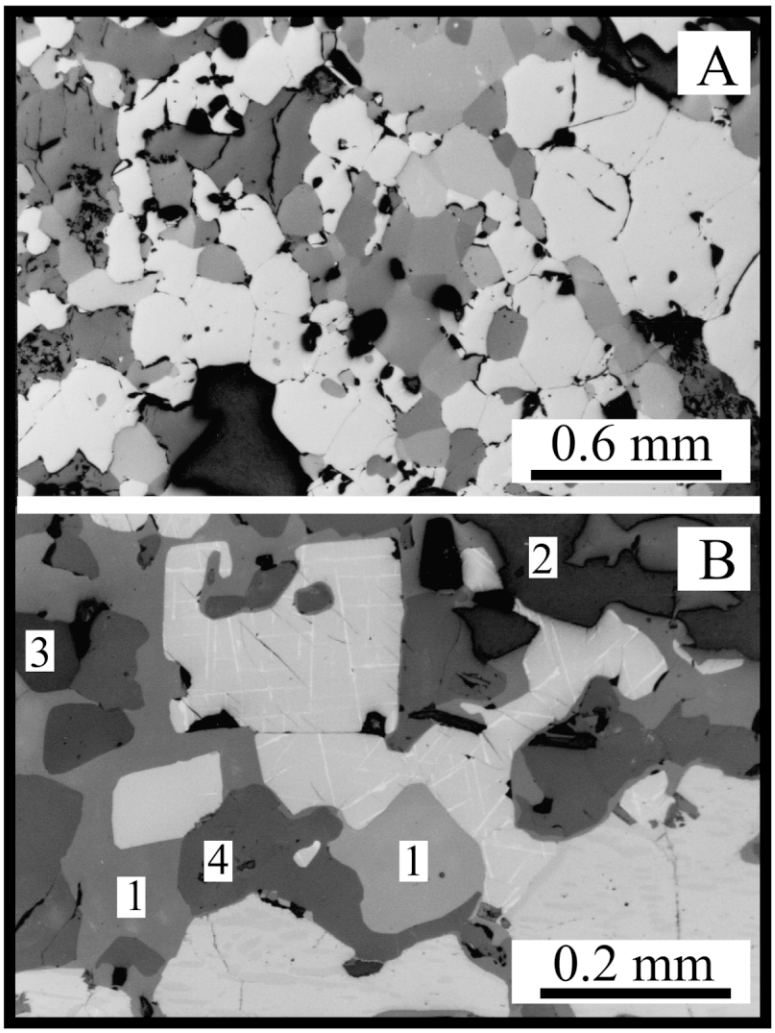

FIG. 3. Reflected-light (plane-polarized) microphotographs of the Fe ore (light grey minerals) and the gangue showing the mosaic textures (A), and an atoll-shape magnetite, containing a garnet inclusion, with hematite arranged in the "martite" texture (B). 1: titanite, 2: chlorite, 3: calcite, 4: garnet.

magnetite has Ti contents varying from 1.06 up to more than 15 wt% TiO_2. Compositions of the green spinel are referable to the general formula $(Fe,Mg)Al_2O_4$ having Fe > Mg (hercynite) or Mg > Fe (spinel *sensu stricto*). Hercynite usually is enriched in Ti and Mn with respect to spinel, and both minerals contain appreciable amounts of Zn (1.79–3.21 wt% ZnO).

The results of electron-microprobe analyses of gangue silicates are presented in Tables 2 and 3. The clinopyroxene has the composition of augite with 1.75–2.32 wt% TiO_2, but no K and Na. The garnet displays an intermediate composition between andradite and grossular, with low Mn (<1.03 wt% MnO) and Ti (<1.86 wt% TiO_2) contents. Titanite has a very low Al contents, between 1.27 and 1.99 wt% Al_2O_3, with an Al/(Ti + Al + Fe) value lower than 0.25. On the basis of Fe/(Fe + Mg) and Si relationships, the chlorite can be classified as Si-poor clinochlore. The brittle mica clintonite has been recognized on the basis of the electron-microprobe data. In the absence of structural data, however, it was not possible to establish the polytype (1*M* or the rare $2M_1$ and 3*A*).

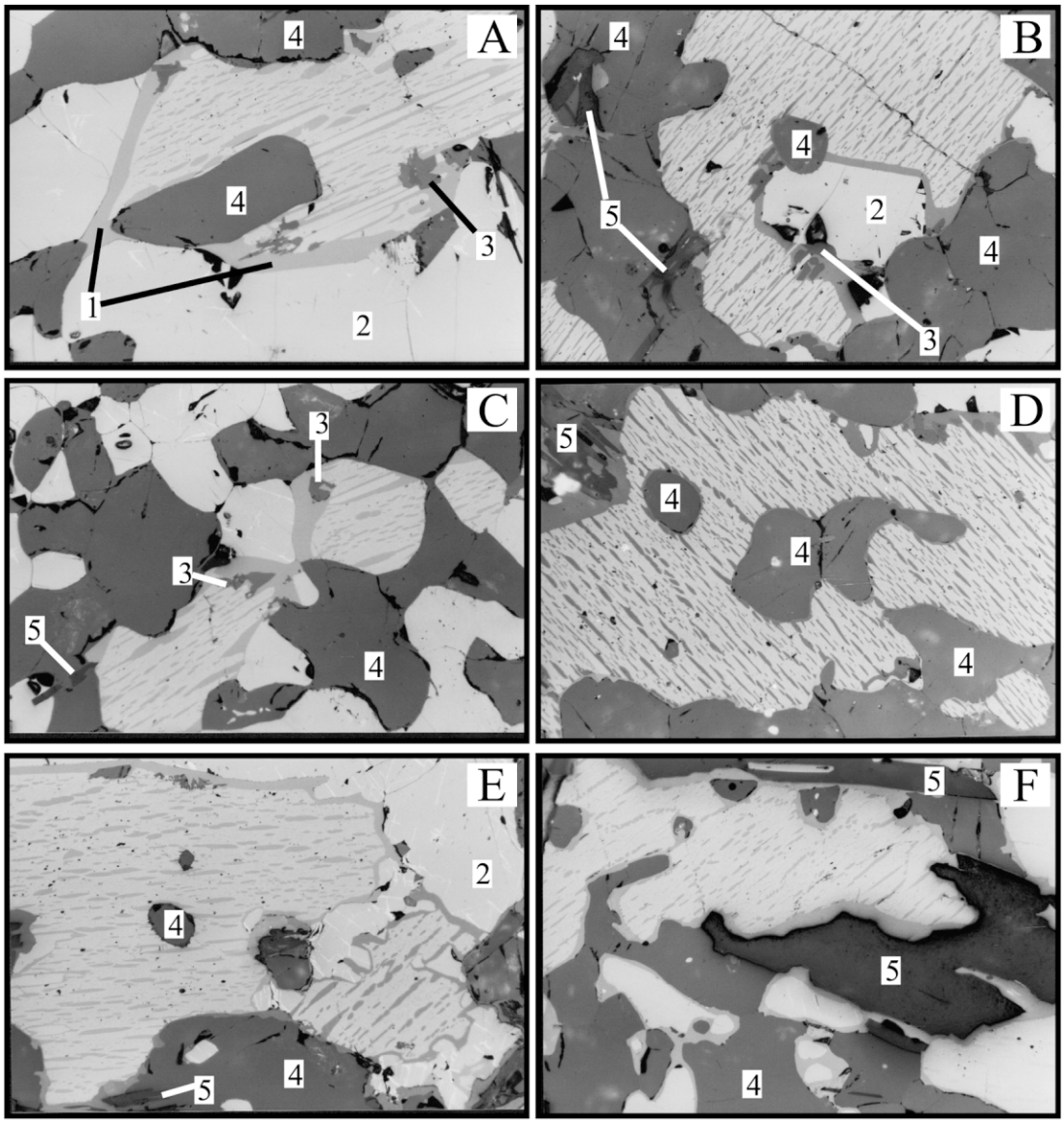

FIG. 4. Reflected-light (plane-polarized) microphotographs of the pyrophanite lamellae and coronas associated with Ti-rich magnetite. The long side of the pictures is 0.55 mm. 1: pyrophanite, 2: Ti-free magnetite (in some cases with hematite lamellae), 3: aluminous spinel, 4: garnet, 5: chlorite.

CHLORITE THERMOMETRY

Chlorite, in most of the investigated samples, occurs as lamellar aggregates intergrown with the ore minerals (Figs 3B, 4), suggesting a common origin. Compositional variations of trioctahedral chlorites are believed to reflect physical–chemical conditions of crystallization. In particular, the amount of ^{IV}Al substituting for Si in the tetrahedral site is temperature-dependent, increasing with depth in hydrothermal, diagenetic or metamorphic systems. The thermometric significance of the analyzed chlorite is not affected by alkali contamination (Frimmel 1997), usually less than 0.1 atom % Ca + Na + K. Treatment of the chlorite data with the equa-

TABLE 1. RESULTS OF SELECTED ELECTRON-MICROPROBE ANALYSES OF OXIDES FROM SIERRA DE COMECHINGONES, ARGENTINA

	SiO_2	TiO_2	Al_2O_3	FeO	Fe_2O_3	MgO	MnO	Cr_2O_3	NiO	ZnO	V_2O_3	Total
Detection limits wt%	0.12	0.03	0.04	0.05	0.05	0.04	0.08	0.05	0.04	0.07	0.02	
Pyrophanite – Ilmenite												
RD5B 1c 1	0.00	54.90	0.04	10.48	0.00	4.97	28.96	0.00	0.00	0.00	0.00	99.35
RD5B 1d 3	0.00	54.58	0.05	11.19	0.00	4.95	28.09	0.00	0.00	0.13	0.00	98.99
RD8A 1 4	0.00	52.45	0.00	6.07	1.05	0.35	39.79	0.00	0.00	0.22	0.27	100.20
RD8A 4 3	0.00	53.93	0.00	19.41	0.70	2.38	24.44	0.00	0.00	0.13	0.13	101.12
RD8A 4 4	0.00	52.43	0.00	21.93	2.33	1.79	21.88	0.00	0.00	0.00	0.24	100.60
RD8A 4 5	0.00	53.35	0.00	20.98	1.40	1.89	23.29	0.06	0.00	0.00	0.22	101.19
RD8A 5 12	0.00	52.66	0.00	7.82	0.00	0.53	37.97	0.00	0.00	0.09	0.36	99.43
RD8A 5 6	0.00	53.73	0.00	20.20	1.12	1.97	24.33	0.00	0.00	0.00	0.51	101.86
RD9A 3a 1	0.00	52.56	0.00	29.38	2.48	3.55	11.30	0.00	0.04	0.01	0.48	99.80
RD9A 3a 10	0.00	51.86	0.00	28.48	3.40	3.60	11.60	0.00	0.07	0.00	0.35	99.36
RD9A 3a 3	0.00	54.23	0.00	30.82	0.00	3.70	11.18	0.00	0.10	0.07	0.16	100.26
RD9A 3b 1	0.00	55.19	0.04	32.59	0.00	3.43	10.43	0.05	0.00	0.00	0.06	101.79
RD9A 3b 2	0.00	54.31	0.04	32.60	0.00	3.28	9.82	0.00	0.01	0.13	0.18	100.37
RD9A 3b 7	0.00	53.87	0.00	30.39	1.65	3.69	11.23	0.00	0.00	0.13	0.09	101.05
RD5B 1b 10	0.00	53.76	0.00	18.22	1.20	5.04	20.90	0.00	0.04	0.00	0.00	99.16
RD5B 1d 1	0.00	54.06	0.00	19.55	0.64	4.83	20.20	0.00	0.00	0.00	0.00	99.28
RD8A 1 2	0.12	53.54	0.00	8.47	0.00	0.43	38.40	0.08	0.00	0.12	0.33	101.49
RD8A 1 3	0.12	53.33	0.00	7.65	0.00	0.38	38.64	0.00	0.04	0.00	0.16	100.32
RD8A 4 10	0.00	52.74	0.00	19.11	2.14	2.37	23.69	0.00	0.00	0.09	0.80	100.94
RD8A 5 11	0.16	52.45	0.00	4.91	0.00	0.21	41.34	0.05	0.00	0.07	0.25	99.44
RD8A 5 14	0.00	52.72	0.00	8.60	0.44	0.83	36.80	0.00	0.13	0.00	0.59	100.11
RD8A 5 15	0.35	51.67	0.16	6.90	1.12	0.57	38.44	0.00	0.00	0.00	0.60	99.81
RD8A 5 16	0.12	52.91	0.00	8.35	0.00	0.65	37.64	0.00	0.00	0.07	0.52	100.26
RD8A 5 2	0.00	54.03	0.00	20.51	0.07	2.21	23.84	0.00	0.00	0.08	0.69	101.43
RD9A 2 3	0.00	52.56	0.00	39.05	3.57	3.00	2.84	0.00	0.00	0.00	0.00	101.02
RD9A 3a 5	0.00	53.29	0.00	30.74	1.92	3.70	10.45	0.00	0.00	0.00	0.25	100.35
RD9A 3b 3	0.00	51.49	0.04	30.37	3.47	3.62	9.39	0.00	0.00	0.00	0.45	98.83
RD9A 3b 8	0.00	54.64	0.04	33.46	0.34	3.29	9.67	0.05	0.00	0.01	0.00	101.50
Spinel – Hercynite												
RD5B 1b 8	0.00	0.29	69.13	6.52	0.00	20.85	1.20	0.00	0.00	3.21	0.03	101.23
RD8A 1 1	0.00	6.11	61.13	17.66	0.00	10.21	1.66	0.06	0.09	1.79	0.09	98.80
RD8A 4 1	0.00	6.63	62.84	16.31	0.00	10.17	1.55	0.00	0.10	1.89	0.07	99.56
RD8A 5 1	1.44	6.32	62.52	16.06	0.00	10.03	1.46	0.00	0.09	2.07	0.13	100.12
RD9A 3a 7	0.00	0.44	68.10	10.62	0.00	19.51	0.82	0.00	0.01	1.92	0.04	101.46
Magnetite												
RD5B 1c 4	0.00	1.26	0.06	30.35	65.54	0.48	0.51	0.05	0.10	0.00	0.12	98.47
RD8A 4 12	0.00	1.18	0.06	31.75	67.13	0.14	0.37	0.00	0.08	0.00	0.29	101.00
RD8A 4 16	0.00	0.05	0.11	30.61	68.45	0.18	0.16	0.10	0.09	0.15	0.26	100.16
RD8A 5 4	0.00	0.14	0.13	30.46	67.98	0.11	0.17	0.00	0.13	0.00	0.26	99.38
RD8A 5 5	0.00	1.42	0.07	32.08	66.69	0.12	0.45	0.09	0.00	0.00	0.25	101.17
RD9A 1 2	0.00	15.17	0.24	44.34	38.97	0.39	0.23	0.09	0.00	0.00	0.20	99.63
RD9A 1 7	0.22	10.16	0.19	40.05	48.08	0.21	0.29	0.09	0.00	0.00	0.32	99.61
RD9A 2 5	0.00	0.19	0.13	29.39	67.90	0.46	0.96	0.05	0.00	0.00	0.29	99.37
RD9A 2	0.00	11.24	0.14	40.40	46.05	0.27	0.26	0.11	0.00	0.00	0.31	98.78
RD9A 3a 4	0.00	1.06	0.05	31.27	65.92	0.13	0.12	0.00	0.13	0.00	0.31	98.99
RD9A 3a 9	0.00	0.03	0.04	30.11	67.64	0.13	0.10	0.07	0.09	0.12	0.29	98.62
RD9A 3b 5	0.38	1.29	0.21	31.68	64.21	0.29	0.10	0.00	0.06	0.00	0.25	98.47
Hematite												
RD8A 4 14	0.00	8.13	0.22	36.60	49.89	0.09	0.67	0.00	0.13	0.15	0.52	96.40
RD8A 4 15	0.00	2.25	0.06	32.32	64.99	0.13	0.64	0.00	0.04	0.28	0.27	100.98

The ferric iron content of the oxide minerals was calculated from ideal stoichiometry.

tion of Cathelineau (1988) yielded results in the range 351–393°C. This range of temperature is shifted toward slightly lower values (300–320°C) if the equation of Kranidiotis & MacLean (1987) is used.

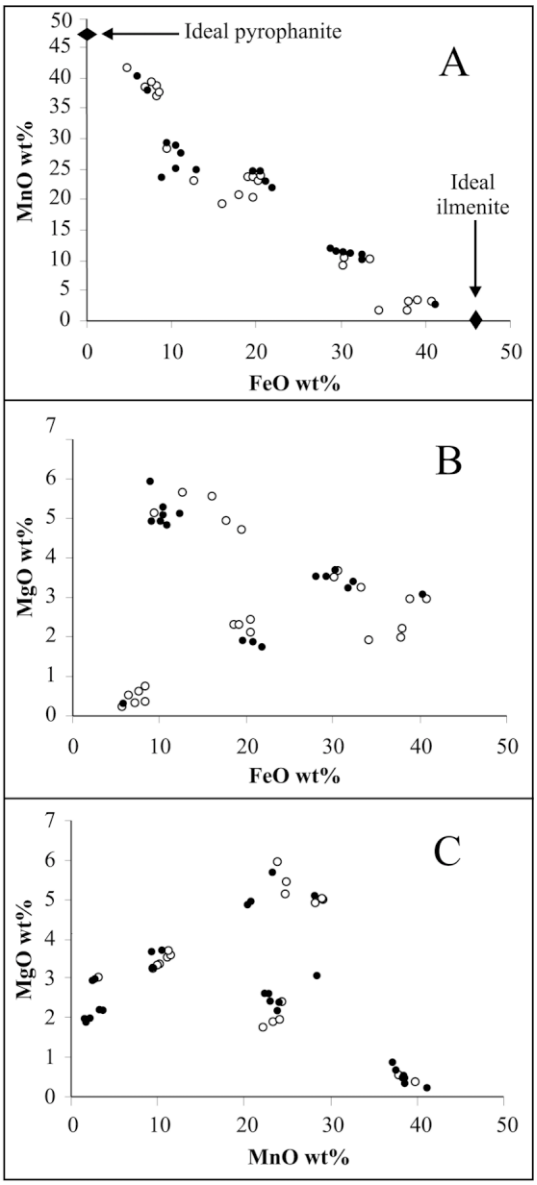

FIG. 5. Reciprocal variations of the major oxides MnO, FeO, and MgO for pyrophanite and manganoan-ilmenite from Sierra de Comechingones (dot: lamellae, open circle: corona).

COMPARISON WITH PYROPHANITE DATA IN THE LITERATURE

The compositions of minerals of the pyrophanite–ilmenite series from Sierra de Comechingones are plotted in terms of FeO–MnO–MgO (Fig. 6), and compared with compositions of pyrophanite and coexisting ilmenite and geikielite taken from the occurrences listed in Table 4, for which chemical data are available. The Mg-poor compositions from Sierra de Comechingones plot along the pyrophanite–ilmenite join together with most compositions from the literature, confirming the existence of a complete solid-solution between the two end members, at negligible or very low contents of the geikielite component (<5% $MgTiO_3$). The Mg-rich compositions from Sierra de Comechingones apparently indicate that the pyrophanite–ilmenite solid solution probably extends to relatively high contents of Mg. These Mg-rich compositions are similar to the members of the pyrophanite–ilmenite series reported from serpentinites of the Kuhmo greenstone belt, Finland (Liipo *et al.* 1994a) and Nigeria (Mücke & Woakes 1986), and carbonatites of the Jacupiranga complex (Gaspar & Wyllie 1983). In most cases, however, the pyrophanite documented in the literature has an Mg content higher than at Sierra de Comechingones, and some compositions from Jacupiranga (Mitchell 1978) and Khumo (Liipo *et al*. 1994b) enter the field of geikielite.

DISCUSSION

Conditions and mechanisms of crystallization of pyrophanite and the associated Fe- and Mg- dominant members of the series can be unequivocally interpreted only in a few cases in the literature. For example, pyrophanite and manganoan ilmenite are believed to have crystallized in equilibrium with granitic melts in the differentiated granitic rocks of the Osumi Peninsula and Kitakami Mountain of Japan (Tsusue 1973, Sasaki *et al*. 2003), in Mont Dore rhyolites, of France (Brousse & Maury 1976), and in the Kuaian granite, in China (Suwa *et al.* 1987). In the last case, pyrophanite was found to contain up to 7.63 wt% ZnO. At Jacupiranga, two types of ilmenite were identified (Gaspar & Wyllie 1983). One consists of discrete primary crystals of pyrophanite and manganoan ilmenite that are considered to have formed at a high temperature during crystallization of the carbonatite, whereas the other occurs as exsolution-induced lamellae in magnetite and is distinctively enriched in Fe and Mg. In a number of other occurrences, members of the pyrophanite–ilmenite series are considered to have formed under metamorphic conditions. For instance, in mafic–ultramafic rocks of Western Australia, manganoan ilmenite can form by diffusion and redistribution of Mn between coexisting oxides and mafic silicates during regional metamorphism (Cassidy *et al.* 1988). In other cases, manganoan

TABLE 2. SELECTED COMPOSITIONS OF SILICATES FROM SIERRA DE COMECHINGONES

	SiO_2	TiO_2	Al_2O_3	FeO	MgO	MnO	CaO	Na_2O	K_2O	Cr_2O_3	Total
Detection limit wt%	0.09	0.02	0.04	0.05	0.04	0.02	0.01	0.02	0.01	0.03	
Clinopyroxene											
RD7s 1 5	42.58	2.32	11.17	7.36	11.44	0.21	25.19	0.00	0.00	0.00	100.27
RD7s 1 7	40.95	1.76	12.18	9.58	10.48	0.19	25.15	0.02	0.00	0.00	100.31
RD9s 1 2	41.38	2.29	12.89	6.94	11.24	0.20	25.08	0.00	0.00	0.00	100.02
RD9s 2 2	43.45	1.74	11.16	6.36	11.63	0.18	25.30	0.00	0.00	0.03	99.85
Garnet											
RD7s 4 1	36.06	1.86	9.17	17.25	0.41	0.87	33.77	0.00	0.00	0.04	99.43
RD7s 4 5	36.56	1.30	10.14	15.83	0.43	1.03	34.19	0.02	0.00	0.03	99.53
RD7s 6 3	36.78	1.58	10.00	16.28	0.48	0.95	33.87	0.00	0.00	0.09	100.03
RD7s 6 8	36.26	1.83	9.53	16.61	0.51	0.91	33.61	0.00	0.00	0.00	99.26
Titanite											
RD7s 1 8	30.41	36.98	1.54	0.86	0.00	0.08	29.15	0.00	0.00	0.03	99.05
RD7s 3 2	30.44	37.12	1.27	1.05	0.00	0.02	29.05	0.02	0.01	0.05	99.03
RD7s 6 5	30.70	36.14	1.99	1.17	0.03	0.04	29.08	0.00	0.01	0.08	99.24
RD7s 8 2	30.12	37.22	1.50	0.92	0.00	0.06	28.96	0.00	0.00	0.00	98.78
Clintonite											
RD9s 3 4	15.66	0.38	41.75	2.78	19.12	0.00	13.54	0.04	0.00	0.00	93.27
RD9s 3 5	15.90	0.34	42.54	2.50	20.54	0.07	13.45	0.08	0.00	0.04	95.46
RD9s 3 6	16.26	0.39	43.21	2.63	19.66	0.03	13.41	0.08	0.00	0.00	95.67
RD9s 3 8	15.25	0.34	42.67	2.69	18.23	0.02	13.52	0.07	0.00	0.06	92.85

TABLE 3. SELECTED COMPOSITIONS OF CHLORITE AND RESULTS OF GEOTHERMOMETRY, METAMORPHIC ASSEMBLAGES OF SIERRA DE COMECHINGONES, ARGENTINA

	SiO_2	TiO_2	Al_2O_3	FeO	MgO	MnO	CaO	Na_2O	K_2O	Cr_2O_3	Total	T °C	
Detection Limit wt%	0.09	0.02	0.04	0.05	0.04	0.02	0.01	0.02	0.01	0.03		*	**
RD7s 4 2	27.95	0.04	23.02	3.72	32.32	0.22	0.03	0.00	0.00	0.00	87.30	376	311
RD7s 4 3	27.87	0.02	23.72	3.93	32.51	0.21	0.03	0.00	0.00	0.00	88.29	387	318
RD7s 4 6	28.73	0.02	22.36	4.30	31.66	0.18	0.02	0.00	0.00	0.00	87.27	351	295
RD7s 6 2	27.61	0.05	22.48	4.18	31.43	0.22	0.02	0.00	0.00	0.03	86.02	371	308
RD7s 6 6	27.55	0.04	22.66	4.27	32.11	0.23	0.04	0.00	0.00	0.04	86.94	381	315
RD7s 7 4	27.65	0.02	22.94	4.04	33.59	0.22	0.04	0.00	0.00	0.00	88.50	393	322
RD9s 1 3	26.40	0.08	22.02	3.89	29.21	0.11	0.04	0.00	0.00	0.00	81.75	369	307
RD9s 3 4	26.93	0.05	23.19	5.18	29.04	0.21	0.04	0.00	0.00	0.00	84.64	376	313
RD9s 4 1	27.34	0.07	21.47	3.96	30.57	0.15	0.03	0.00	0.00	0.00	83.59	357	299

Geothermometer: * Cathelineau (1988), ** Kranidiotis & MacLean (1987).

and magnesian ilmenite, locally reaching the composition of pyrophanite and geikielite, are formed by reaction of ultramafic rocks with hydrothermal fluids (Liipo *et al.* 1994a).

The pyrophanite and manganoan ilmenite from Sierra de Comechingones are metamorphic minerals. The textural relationships suggest that both phases and their Ti-rich magnetite host formed by unmixing from a (Fe,Ti)-oxide precursor, the composition of which is probably referable to a member of the magnetite–ulvöspinel solid solution, although with substantial substitution of Mn and Mg for Fe^{2+}, and containing minor amounts of Al and Zn. According to experimental data (Buddington & Lindsley 1964), the solubility of ilmenite in magnetite is too limited to account for the formation of lamellae assemblages such as those de-

scribed here, by simple subsolidus exsolution. The large volume of ilmenite lamellae inside magnetite requires that the magnetite–ulvöspinel precursor underwent oxidation-induced reactions under metamorphic conditions.

The presence of Mn and Mg in the magnetite–ulvöspinel precursor led to the formation of pyrophanite and manganoan ilmenite containing appreciable geikielite component at Sierra de Comechingones. In other occurrences associated with metamorphosed mafic–ultramafic rocks, it has been proposed that Mn and Mg might have been added to the oxide-forming system from an external source by metamorphic diffusion or reaction with hydrothermal fluids. In our case, the composition of the gangue silicates suggests that such a

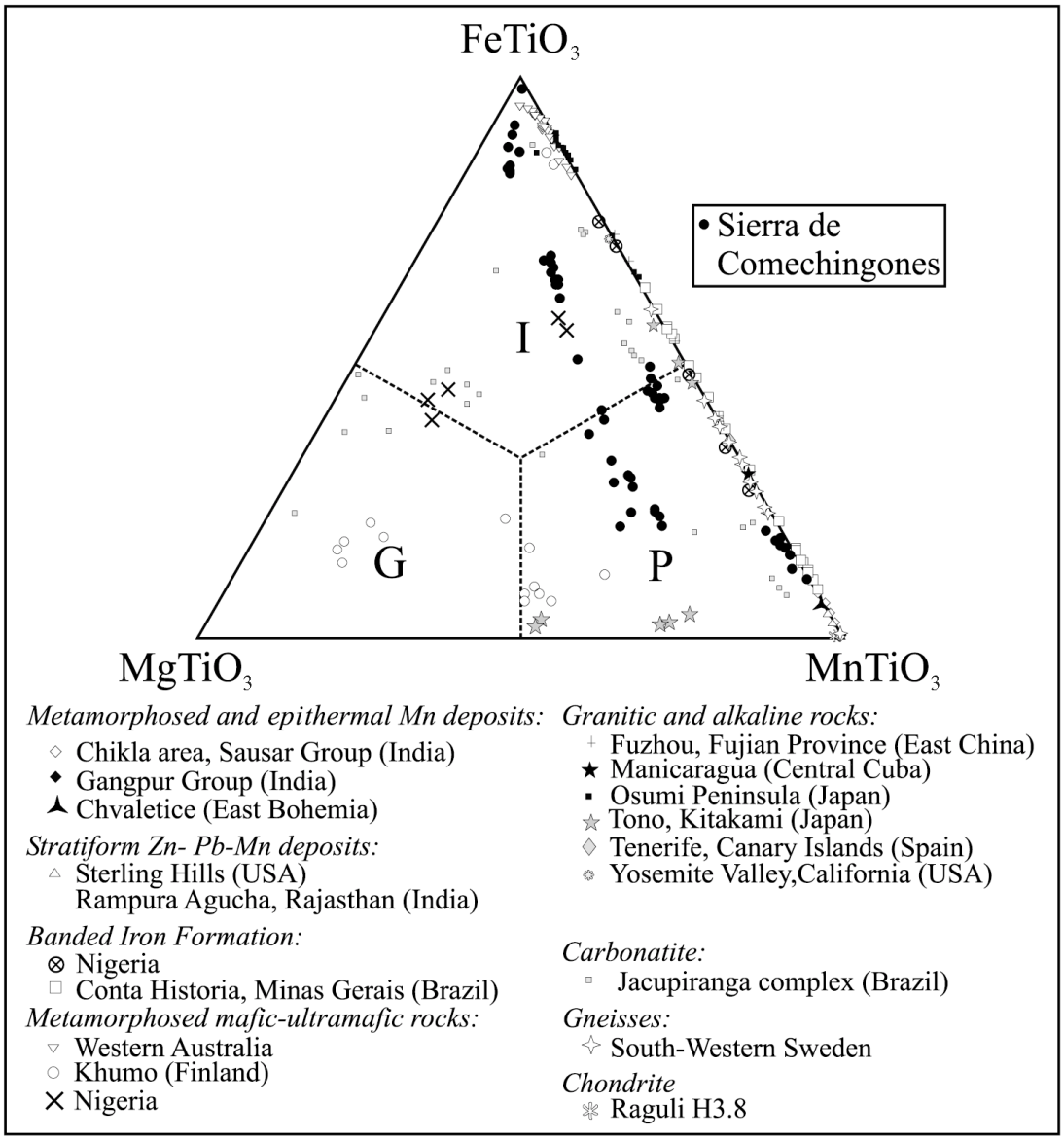

FIG. 6. Compositions of pyrophanite and manganoan ilmenite of Sierra de Comechingones plotted in the system $FeTiO_3$–$MnTiO_3$–$MgTiO_3$. Compositional data from the literature are shown for comparison (see Table 4 for references). Fields of pyrophanite (P), ilmenite (I) and geikielite (G) are shown.

TABLE 4. SELECTED WORLD-WIDE OCCURRENCES OF PYROPHANITE

Country	Location	Deposits	Type of Deposits	Host Rock	Origin of Pyrophanite	Ref.
India	Rajasthan		Stratiform Pb–Zn	Metasedimentary rocks	Exsolution at low T,P from rutile	1
	Maharashtra State	Chikla	Metamorphosed Mn	Quartz-rich metamorphic rocks	Exsolution at high $f(O_2)$	2
	Gangpur	Nishikal	Metamorphosed Mn			3, 4
	Goriajhar Region		Metamorphosed Mn	Gondite	Metamorphic	5
Japan	Chichibu Complex	Ajiro, Kinko, Kusugi, Noda, Tamagawa, Renge		Chert		6
		Kitakami Mtn.		Granitic rocks	Magmatic differentiation	7
	Osumi Peninsula			Granite	Magmatic differentiation	8
China	Fuzhou, Fujian Province	Kuaian		Granite	Magmatic	9
USA	New Jersey	Sterling Hill	Stratiform Zn–Fe–Mn	Marble	Metamorphic and oxidation-induced exsolution	10, 11
	North Carolina	Bald Knob	Metamorphosed Mn	Metasedimentary rocks		12, 13
	Idaho, Sawtooth			Granite		14
	California			Quarz-rich adamellite	Magmatic differentiation	15
Canada	Quebec	Mont Saint-Hilaire		Alkaline complex		16
Cuba	Manicaragua Zone			Granitic rocks	Magmatic, metamorphic	17
Brazil	Minas Gerais	Conta Historia	Banded iron-formation	Itabirite and dolomite	Metamorphic and hydrothermal	18
	Jacupiranga			Carbonatites	Magmatic and fluid-based reaction	19
Ghana	Eburnean Province			Gondite	Premetamorphic	20
Nigeria			Serpentinites, banded iron-formation		Metamorphic	21
Spain	Tenerife, Canary Is.			Nepheline syenite		22
France	Charlannes, Mont-Dore			Alkaline rhyolite	Magmatic differentiation	23
Italy	Val Graveglia	Gambatesa	Hydrothermal Mn			24, 25
Finland	Ensila, Kuhmo			Serpentinized wehrlite	Metamorphic and hydrothermal	26, 27
Sweden				Gneisses		28
Czech Rep.	Iron Mountain	Chvaletice	Pyrite–Mn	Metamorphosed carbonates	Hydrothermal metamorphism	29
Romania	Semenic Mtns.	Delinesti	Epithermal Mn	Metamorphic rocks	Post-metamorphic	30
	Bistrita Mtns.	Oita	Metamorphosed Mn	Mn carbonates-silicates	Metamorphic	31
Russia	North Baikalia	Burpala	Alkaline complex			32, 33
Australia		Broken Hill		Stratiform Pb–Zn		34

References: 1: Holler & Gandhi (1997)*, 2: Dasgupta *et al.* (1984)*, 3: Acharya *et al.* (1997), 4: Rao *et al.* (1994)*, 5: Nayak & Mohapatra (1998), 6: Lee (1955), 7: Sasaki *et al.* (2003)*, 8: Tsusue (1973)*, 9: Suwa *et al.* (1987)*, 10: Craig *et al.* (1985)*, 11: Valentino *et al.* (1990), 12: Simmons *et al.* (1981), 13: Winters *et al.* (1981), 14: Menzies & Boggs (1993), 15: Snetsinger (1969), 16: Horváth & Gault (1990), 17: Ulrych & Lang (1985)*, 18: Cabral & Sattler (2001)*, 19: Gaspar & Wyllie (1983)*, 20: Melcher (1995), 21: Mücke & Woakes (1986)*, 22: Ferguson (1978)*, 23: Brousse & Maury (1976), 24: Marchesini & Pagano (2001), 25: Palenzona (1996), 26: Liipo *et al.* (1994a)*, 27: Liipo *et al.* (1994b)*, 28: Lindh & Malmstrom (1984), 29: Zak (1971)*, 30: Hartopanu *et al.* (1995), 31: Perseil *et al.* (1995), 32: Portnov (1965), 33: Portnov (2001), 34: Mason (1976). * : Chemical data available and plotted in Figure 5.

process may hold for Mg, but does not fit for Mn, since this element is present only in andradite–grossular at concentrations lower than 1.03 wt% MnO. Therefore, we suggest that Mn was probably present in the Fe oxide of the original protolith. The nature of the protolith at Sierra de Comechingones and its metamorphic evolution are so far unclear, and will be the subject of further investigation.

Concluding Remarks

1) Metamorphosed Fe ore in Sierra de Comechingones, Argentina, contains pyrophanite and manganoan ilmenite as exsolution lamellae inside Ti-rich magnetite. The Ti-rich magnetite coexists, at the thin section scale, with Ti-free magnetite.

2) The microprobe-derived compositions presented here, together with literature data, document the existence of extensive solid-solution among the end members: pyrophanite ($MnTiO_3$), ilmenite ($FeTiO_3$), and geikielite ($MgTiO_3$).

3) Textural and compositional relationships support the hypothesis that the unmixing assemblage pyrophanite–magnetite may have been derived by equilibration of a precursor Mn–Mg-rich magnetite–ulvöspinel solid solution.

4) The lack of Mn in the silicate minerals associated with the Fe ore seems to exclude the possible influx of Mn-rich fluids during metamorphism, and suggests instead that Mn was an important constituent of the original oxide protolith.

5) The lowest temperatures, obtained from chlorite, vary from 300 to 351°C, possibly consistent with the closure of the metamorphic system. However, textural and mineralogical evidence suggest that the metamorphic temperature was much higher and possibly reached a stage of partial melting. The high-temperature Mn–Mg-rich magnetite–ulvöspinel solid solution that was the precursor to the exsolution assemblage pyrophanite – manganoan ilmenite – Ti-rich magnetite possibly formed from such a molten fraction, coexisting with a residual Ti-free magnetite (R.F. Martin, pers. commun.).

6) This is the first documented occurrence of pyrophanite and clintonite in Argentina.

Acknowledgements

The authors are grateful to Prof. Carlos Costa, Universidad Nacional de San Luis (Argentina), for support during the field activities. We greatly acknowledge the constructive comments by Alexandre Cabral and Raul Lira. Special thanks are due to Robert F. Martin for his useful suggestions and revision of the English text. The Italian authors are grateful to the MIUR (COFIN 2001, Leader: Prof. C. Cipriani) for financial help.

References

Acharya, B.C., Rao, D.S. & Sahoo, R.K. (1997): Mineralogy, chemistry and genesis of Nishikhal manganese ores of South Orissa, India. *Mineral. Deposita* **32**, 79-93.

Brousse, R. & Maury, R.C. (1976): Paragenèse manganésifère d'une rhyolite hyperalcaline du Mont-Dore. *Bull. Soc. Fr. Minéral. Cristallogr.* **99**, 300-303.

Buddington, A.F. & Lindsley, D.H. (1964): Iron–titanium oxide minerals and synthetic equivalents. *J. Petrol.* **5**, 310-317.

Cabral, A.R. & Sattler, C.D. (2001): Contrasting pyrophanite–ilmenite solid compositions from the Conta Historia Fe–Mn deposits, Quadrilatero Ferrifero, Minas Gerais, Brazil. *Neues Jahrb. Mineral., Monatsh.*, 271-288.

Cassidy, K.F., Groves, D.I. & Binns, R.A. (1988): Manganoan ilmenite formed during regional metamorphism of Archean mafic and ultramafic rocks from Western Australia. *Can. Mineral.* **26**, 999-1012.

Cathelineau, M. (1988): Cation site occupancy in chlorites and illites as a function of temperature. *Clay Minerals* **23**, 471-485.

Craig, J.R., Sandhaus, D.J. & Guy, R.E. (1985): Pyrophanite $MnTiO_3$ from Sterling Hill, New Jersey. *Can. Mineral.* **23**, 491-494.

Dasgupta, S., Fukauaki, M. & Roy, S. (1984): Hematite–pyrophanite intergrowth in gondite, Chikla area, Sausar Group, India. *Mineral. Mag.* **48**, 555-560.

Derby, A.O. (1901): On the manganese ore deposits of the Queluz (Lafayette) District, Minas Geraes, Brazil. *Am. J. Sci.* **162**, 18-32.

_____ (1908): On the original type of the manganese ore deposits of the Queluz District, Minas Geraes, Brazil. *Am. J. Sci.* **175**, 213-216.

Donovan, J.J. & Rivers, M.L. (1990): PRSUPR – a PC based automation and analyses software package for wavelength dispersive electron beam microanalysis. *Microbeam Anal.*, 66-68.

Ferguson, A.K. (1978): The occurrence of ramsayite, titanlåvenite and fluorine-rich eucolite in a nepheline-syenite inclusion from Tenerife, Canary Islands. *Contrib. Mineral. Petrol.* **66**, 15-20.

Frimmel, H.E. (1997): Chlorite thermometry in the Witwatersrand Basin: constraints on the Palaeoproterozoic geotherm in the Kaapvaal Craton, South Africa. *J. Geol.* **105**, 601-615.

Gaspar, J.C. & Wyllie, P.J. (1983): Ilmenite (high Mg, Mn, Nb) in the carbonatites from the Jacupiranga Complex, Brazil. *Am. Mineral.* **68**, 960-971.

GORDILLO, C. & LENCINAS, H. (1979): Las Sierras Pampeanas de Córdoba y San Luis. *II Simposio de Geología Regional Argentina. Academia Nacional de Ciencias* **I**, 577-650.

GUERESCHI, A.B. (2000): Estructura y petrología del basamento metamórfico del flanco oriental de la Sierra de comechingones, pedanías Cañada de Alvarez y Río de Los Sauces, departamento Calamuchita, provincia de Córdoba, Argentina. Tesis Doctoral, Universidad Nacional de Córdoba, Córdoba, Argentina.

_____ & BALDO, E.G. (1993): Petrología y geoquímica de las rocas metamórficas del sector centro-oriental de la Sierra de Comechingones, Córdoba. 12° Congreso Geológico Argentino y 2° Congreso de Exploración de Hidrocarburos (Mendoza) **4**, 319-325.

_____ & MARTINO, R. (2002): Geotermometría de la paragénesis Qtz + Pl + Bt + Grt + Sil en gneises de alto grado del sector centro-oriental de la Sierra de Comechingones, Córdoba. *Rev. As. Geol. Argentina* **57**, 365-375.

_____ & _____ (2003): Trayectoria textural de las metamorfitas del sector centro-oriental de la Sierra de Comechingones, Córdoba. *Rev. As. Geol. Argentina* **58**, 61-77.

HAMBERG, A. (1890): Über die Manganophylle von der Grube Harstingen bei Pajsberg in Vermland. 10. Über Pyrophanit, eine mit dem Titaneisen isomorphe Verbindung der Zusammensetzung $MnTiO_3$, von Harstigen. *Geol. Fören. Stockholm Förh.* **12**, 598-604.

HARTOPANU, P., CRISTEA, C. & STELA, G. (1995): Pyrophanite of Delinesti (Semenic Mountains). *Rom. J. Mineral.* **77**, 19-24.

HOLLER, W. & GANDHI, S.M. (1997): Origin of tourmaline and oxide minerals from the metamorphosed Rampura Agucha Zn–Pb–(Ag) deposit, Rajasthan, India. *Mineral. Petrol.* **60**, 99-119.

HORVATH, L. & GAULT, R.A. (1990): The mineralogy of Mont Saint Hilaire, Quebec. *Mineral. Rec.* **21**, 284-359.

ISACKS, B. (1988): Uplift of the central Andean plateau and bending of the Bolivian Orocline. *J. Geophys. Res.* **B93**, 3211-3231.

JORDAN, T.E. & ALLMENDINGER, R.W. (1986): The Sierras Pampeanas of Argentina: a modern analogue of Rocky Mountain foreland deformation. *Am. J. Sci.* **286**, 737-764.

KRAEMER, P.E., ESCAYOLA, M.P. & MARTINO, R.D. (1995): Hipótesis sobre la evolución tectónica neoproterozoica de las Sierras Pampeanas de Córdoba (30°40' – 32°40'). *Revista de la Asociación Geológica Argentina* **50**, 47-59.

KRANIDIOTIS, P. & MACLEAN, W.H. (1987): Systematics of chlorite alteration at the Phelps Dodge massive sulfide deposit, Matagami, Quebec. *Econ. Geol.* **82**, 1898-1911.

KROT, A.N., RUBIN, A.E. & KONONKOVA, N.N. (1993): First occurrence of pyrophanite ($MnTiO_3$) and baddeleyite (ZrO_2) in an ordinary chondrite. *Meteoritics* **28**, 232-252.

LEE, D.E. (1955): Occurrence of pyrophanite in Japan. *Am. Mineral.* **40**, 32-40.

LINDH, A. & MALMSTROM, L. (1984): The occurrence and formation of pyrophanite in late-formed magnetite porphyroblasts. *Neues Jahrb. Mineral., Monatsh.*, 13-21.

LIIPO, J.P., VUOLLO, J.I., NYKANEN, V.M. & PIIRAINEN, T.A. (1994a): Pyrophanite and ilmenite in serpentinized wehrlite from Ensilia, Kuhmo greenstone belt, Finland. *Eur. J. Mineral.* **6**, 145-150.

_____, _____, _____ & _____ (1994b): Geikielite from the Naataniemi serpentinite massif, Kuhmo greenstone belt, Finland. *Can. Mineral*. **32**, 327-332.

MARCHESINI, M. & PAGANO, R. (2001): The Val Graveglia manganese district, Liguria, Italy. *Mineral. Rec.* **32**, 349-415.

MASON, B. (1976): Famous mineral localities: Broken Hill, Australia. *Mineral. Rec.* **7**, 25-33.

MELCHER, F. (1995): Genesis of chemical sediments in Birimian greenstone belts: evidence from gondites and related manganese-bearing rocks from northern Ghana. *Mineral. Mag.* **59**, 229-251.

MENZIES, M.A. & BOGGS, R.C. (1993): Minerals of the Sawtooth batholith. Idaho. *Mineral. Rec.* **24**, 185-202.

MITCHELL, R.H. (1978): Manganoan magesian ilmenite and titanian clinohumite from the Jacupiranga carbonatite, Sao Paulo, Brazil. *Am. Mineral.* **63**, 544-547.

MÜCKE, A. & WOAKES, M. (1986): Pyrophanite: a typical mineral in the Pan-African province of western and central Nigeria. *J. Afr. Earth Sci.* **5**, 675-689.

NAYAK, B.R. & MOHAPATRA, B.K. (1998): Two morphologies of pyrophanite in Mn-rich assemblages, Gangpur Group, India. *Mineral. Mag.* **62**, 847-856.

PALENZONA, A. (1996): I nostri minerali: geologia e mineralogia in Liguria, aggiornamento 1995. *Rivista Mineral. Italiana* **2**, 149-172.

PERSEIL, E.A., GIOVANOLI, R. & VODA, A. (1995): Evolution minéralogique du manganèse dans les concentrations de Oita (Monts de Bistrita). Carpates Orientales, Roumanie. *Rom. J. Mineral.* **77**, 11-18.

PETAEV, M.I., ZASLAVSKAYA, N.I., CLARKE, R.S., OLSEN, E.J., JAROSEWICH, E., KONONKOVA, N.N., HOLMBERG, B., DAVIS, A.M., USTINOV, V.I. & WOOD, J.A. (1992): The Chaunskij meteorite: mineralogical, chemical and isotope data, classification and proposed origin. *Meteoritics* **27**, 276-277.

PORTNOV, A.M. (1965) Pyrophanite from northern Baikalia. *Dokl. Acad. Sci. USSR, Earth Sci. Sect.* **153**, 126-138.

_____ (2001): Mineralogy of the Burpala alkaline massif (north of lake Baikal). *Mineral. Rec.* **32**, 42.

RAO, D.S., ACHARYA, B.C. & SAHOO, R.K. (1994): Pyrophanite from Nishikal manganese deposits, Orissa. *J. Geol. Soc. India* **44**, 91-93.

RAPELA, C.W., PANKHURST, R.J., CASQUET, C., BALDO, E., SAAVEDRA, J., GALINDO, C. & FANNING, C.M. (1998): The Pampean Orogeny of the southern proto-Andes: Cambrian continental collision in the Sierras de Córdoba. *In* The Proto-Andean Margin of Gondwana (R. Pankhurst & C. Rapela, eds.). *Geol. Soc. London, Spec. Publ*. **142**, 181-217.

SASAKI, K., NAKASHIMA, K. & KANISAWA, S. (2003): Pyrophanite and high Mn ilmenite discovered in the Cretaceous Tono pluton, NE Japan. *Neues Jahrb. Mineral., Monatsh.*, 302-320.

SIMMONS, W.B., JR., PEACOR, D.R., ESSENE, E.J. & WINTER, G.A (1981): Manganese minerals of Bald Knob, North Carolina. *Mineral. Rec.* **12**, 167-171.

SIMS, J.P., IRELAND, T.R., CAMACHO, A. , LYONS, P., PIETERS, P.E., SKIRROW, R., STUART-SMITH, P.G. & MIRÓ R. (1998): U–Pb, Th–Pb and Ar–Ar geochronology from the southern Sierras Pampeanas, Argentina: implications for the Palaeozoic tectonic evolution of the western Gondwana margin. *In* The Proto-Andean Margin of Gondwana (R. Pankhurst & C. Rapela, eds.). *Geol. Soc. London, Spec. Publ*. **142**, 259-281.

SMITH, W.C. & CLARINGBULL, G.F. (1947): Pyrophanite from the Benalt mine, Rhiw, Carnavonshire. *Mineral. Mag.* **28**, 108-110.

SNETSINGER, K.G. (1969): Manganoan ilmenite from a Sierran adamellite. *Am. Mineral.* **54**, 431-436.

SUWA, K., ENANI, M., HIRAIWA, I. & YANG, T. (1987): Zn–Mn ilmenite in the Kuiqi granite from Fuzhou, Fujian province, East China. *Mineral. Petrol.* **36**, 111-120.

TSUSUE, A. (1973): The distribution of manganese and iron between ilmenite and granitic magma in the Osumi Peninsula, Japan. *Mineral. Petrol.* **40**, 305-314.

ULRYCH, J. & LANG, M. (1985): Accessory pyrophanite in granite and manganojacobsite in dioritic amphibolite from the Manicaragua Zone, central Cuba. *Chemie der Erde* **44**, 273-280.

VALENTINO, A.J., CARVALHO, A.V., III & SCLAR, C.B. (1990): Franklinite – magnetite – pyrophanite intergrowths in the Sterling Hill zinc deposits, New Jersey. *Econ. Geol.* **85**, 1941-1946.

WINTER, G.A, ESSENE, E.J. & PEACOR, D.R. (1981): Carbonates and pyroxenoids from the manganese deposit near Bald Knob, North Carolina. *Am. Mineral.* **66**, 278-289.

ZAK, L. (1971): Pyrophanite from Chaevaletice (Bohemia). *Mineral. Mag.* **38**, 312-316.

Received August 29, 2003, revised manuscript accepted December 3, 2003.